

# Comparison of Magnetic Resonance Imaging Sequences With Computed Tomography to Detect Low-Grade Subarachnoid Hemorrhage

## Role of Fluid-Attenuated Inversion Recovery Sequence

Antônio José da Rocha, MD,\* Carlos Jorge da Silva, MD,\* Hugo Pereira Pinto Gama, MD,\*  
Carlos Eduardo Baccin, MD,\* Flávio Túlio Braga, MD,\* Fabiane de Araújo Cesare, MD,†  
and José Carlos Esteves Veiga, MD†

**Objectives:** To compare computed tomography (CT) with magnetic resonance imaging (MRI) for the presumptive diagnosis and localization of acute and subacute low-grade subarachnoid hemorrhage (SAH).

**Methods:** We consecutively enrolled 45 patients clinically suspected of low-grade SAH, comparing them with a control group. We obtained axial nonenhanced CT scans as well as fluid-attenuated inversion recovery (FLAIR) and T2-weighted gradient echo (T2\*) MRI sequences at 1.0 T. Two neuroradiologists scrutinized the presence of blood at 26 different regions in the intracranial subarachnoid space (SAS).

**Results:** Three of 45 patients had normal CT and MRI scans, and SAH was excluded by lumbar puncture. We demonstrated SAH on CT scans in 28 of 42 (66.6%) patients, T2\* sequences in 15 of 42 (35.7%) patients, and FLAIR sequences in 42 of 42 (100%) patients. Fluid-attenuated inversion recovery sequences were superior to CT in 16 of the 26 evaluated regions.

**Conclusions:** The FLAIR sequence was superior for presumptive diagnosis and localization of acute and subacute low-grade SAH, representing a potential tool in this setting.

**Key Words:** computed tomography, magnetic resonance imaging, subarachnoid hemorrhage, headache, subarachnoid space

(*J Comput Assist Tomogr* 2006;30:295–303)

Subarachnoid hemorrhage (SAH) is an important neurologic emergency, mainly in nontraumatic cases, with a catastrophic outcome if left untreated.<sup>1</sup> Trauma is the most common cause of SAH, and a ruptured aneurysm counts for most nontraumatic SAH.<sup>2,3</sup>

The clinical presentation of spontaneous SAH includes severe sudden headache (frequently described as “the worst headache of my life”), nuchal rigidity, photophobia, vomiting, retinal hemorrhage, diminished level of consciousness, focal neurologic signs, and a comatose state. Early diagnosis is important so as to initiate therapeutic procedures to avoid vasospasm, rebleeding, and hydrocephalus, improving patient prognosis.<sup>1–3</sup> It is also important to distinguish SAH attributable to a ruptured aneurysm from benign thunderclap headache and other neurologic conditions that could simulate SAH based on clinical grounds.<sup>1,4,6</sup> Despite the widespread availability of neuroimaging equipment, misdiagnosis of SAH remains quite common.<sup>1–3</sup> Thus, it is a potential cause of litigation and poor prognosis.<sup>2,4</sup>

Computed tomography (CT) has been the imaging procedure of choice in cases of suspected SAH.<sup>2,7</sup> Currently, lumbar puncture is performed if the patient’s history is suggestive of SAH and CT results are normal. The sensitivity of CT to SAH is more than 90% at the first day but falls off rapidly with time and approaches 0% at 3 weeks.<sup>7,8</sup> Moreover, CT results are unreliable in cases of minor hemorrhage, mainly in the infratentorial compartment.<sup>9</sup> It has been assumed that those misdiagnosed patients with minor hemorrhage and good clinical conditions at presentation are more likely to deteriorate clinically and have a worse overall outcome, particularly because of the delay in diagnosis and subsequent catastrophic rebleeding from a ruptured aneurysm.<sup>1,3,6,10</sup>

Magnetic resonance imaging (MRI) shows high sensitivity and accuracy in the diagnosis of a wide variety of central nervous system diseases. It is accepted that T1- and T2-weighted sequences are limited and less informative for SAH than CT, however. Initially, Chakeres and Bryan<sup>11</sup> proved that CT has an imaging advantage, because high-concentration hemorrhage is clearly different from the normal brain, whereas concentrated acute SAH has relaxation times similar to normal brain and is nearly isointense on T1- and T2-weighted MRI sequences. Atlas<sup>12</sup> reviewed the literature in the early 1990s and concluded that MRI was not accurate in detecting SAH. After that, a few reports have demonstrated that MRI can detect SAH if fluid-attenuated inversion recovery (FLAIR)<sup>13–15</sup> and T2-weighted gradient-echo (T2\*)<sup>16</sup> images are used. The appropriate use of MRI to

Received for publication September 24, 2005; accepted November 30, 2005.  
From the \*Section of Radiology, Santa Casa de Misericórdia de São Paulo, São Paulo, Brazil, and †Section of Neurosurgery, Santa Casa de Misericórdia de São Paulo, São Paulo, Brazil.

Reprints: Dr. Carlos Jorge da Silva, Centro de Medicina Diagnóstica-Setor de Imagem Laboratório, Fleury Rua Cincinato Braga, 282 Paraíso, CEP 01333910, São Paulo-SP, Brazil (e-mail: carlos.silva@fleury.com.br).  
Copyright © 2006 by Lippincott Williams & Wilkins

detect low-grade SAH remains controversial and needs further confirmation.

Our aim is to compare the sensitivity of MRI (FLAIR and T2\* sequences) with CT scans for the presumptive diagnosis and localization of acute and subacute low-grade SAH and to try to establish preliminary parameters for the interpretation of these techniques in this setting.

## MATERIALS AND METHODS

From September 2002 to May 2003, we consecutively enrolled 45 patients with clinically suspected low-grade SAH, within the first 15 days of symptoms, at the Emergency Division of our institution. We initially divided these patients into 2 groups: traumatic and spontaneous SAH. The inclusion criteria for the traumatic SAH group were previously healthy individuals with head injury, a Glasgow Coma Scale score greater than 9, and clinically suspected SAH. The inclusion criteria for the spontaneous SAH group were severe headache that led to suspicion of SAH, with minimal clinical abnormalities (Hunt-Hess scale score <3). The exclusion criteria for both groups were patients with deteriorating clinical conditions, patients suspected of meningeal affections, extensive SAH detected on nonenhanced CT scans, restriction to MRI examinations, and images with movement artifacts. Neither sedation nor anesthesia was performed in any of our patients.

Forty-five patients, 25 male (55.5%) and 20 female (44.5%), were included, given those criteria, with an age range from 1 to 80 years (mean = 39.5 years), and a Glasgow Coma Scale score range from 10 to 15 (mean = 14). Three (6.66%) of those patients were excluded because they had no signs of SAH on CT and MRI examinations, as confirmed by a negative result on lumbar puncture. Thus, we selected a group of 42 patients who had SAH as shown by symptoms and 1 imaging technique at a minimum.

Twenty-five of 42 (59.5%) patients were in the traumatic SAH group, and the remaining 17 (40.5%) patients were in the spontaneous group (15 with ruptured aneurysms, 1 with a right intracranial vertebral artery dissection, and 1 with thrombocytopenia attributable to chronic myelogenous leukemia).

We performed all examinations within 2 hours to 15 days after the ictus or trauma, and to avoid rebleeding effects in the spontaneous SAH group, we obtained the CT scans less than 2 hours after the MRI examinations. In 4 cases in which this was not possible, we obtained a second CT scan less than 2 hours after the MRI examination.

For statistical analysis, we divided the patients into an acute group (32 individuals scanned less than 4 days after the ictus or trauma) and a subacute group (10 individuals scanned within 4 to 15 days after these events). The control group consisted of 21 patients (11 women) with a mean age of 49.9 years (age range: 26–70 years) and without clinically suspected SAH or other meningeal conditions.

We performed axial nonenhanced CT scans (20-cm field of view, 5-mm infratentorial thickness, 10-mm supratentorial thickness, and 320 × 320 matrix) in all patients except the control group. Magnetic resonance imaging examinations at 1.0 T were performed in all patients. After 3 localizing scans

in the axial, coronal, and sagittal planes, axial slices covering the whole brain were aligned with the bicommissural line. Imaging parameters were identical (24-cm field of view, 5-mm thickness, 0.3-mm gap, and 205 × 512 matrix). Our protocol included axial FLAIR (repetition time=11,000 milliseconds, echo time = 140 milliseconds, inversion time = 2600 milliseconds) and T2\* (repetition time = 615 milliseconds, echo time = 21 milliseconds, and 15° flip angle) sequences. The total scanning time was approximately 8 minutes for each patient. We routinely perform brain digital angiography in all patients with spontaneous SAH.

Informed consent was obtained from all subjects, and this protocol was approved by the Institutional Review Board. Appropriate clinical care was dispensed to subjects according to individual needs, and none of them demonstrated any clinical deterioration during their hospitalization.

Two experienced neuroradiologists (AJR, FTB), blinded to clinical data, analyzed CT and MRI examinations of each patient independently. The films were presented in random order (not sequential), without identification. Computed tomography and MRI studies were not presented together, and the presence of SAH was searched for separately, in a systematized analysis, in the following 26 locations: magna, prepontine, superior cerebellar, perimesencephalic, interpeduncular, suprasellar, and right and left cerebellopontine cisterns; cerebellar sulci; right and left tentorium; frontal, parietal, and occipital interhemispheric sulci; right and left frontal, parietal, temporal and occipital convexity sulci; right and left convexity sulci; and right and left Sylvian fissures.

We visually defined SAH based on high-attenuation areas on nonenhanced CT scans, regions of hyperintensity on FLAIR sequences, and regions of hypointensity on T2\* sequences, located in the previously mentioned subarachnoid space (SAS). Disagreement between the 2 neuroradiologists was solved by consensus.

To compare the methods (FLAIR imaging, T2\* imaging, and CT), the amount of SAH was graded according to a modified Fisher grade for vasospasm<sup>17</sup> as follows: 0 indicates no blood detected, 1 indicates uncertain appearance (probable artifact but unable to exclude small focal hemorrhage completely), 2 indicates diffuse deposition or thin vertical layers of blood less than 1 mm thick, and 3 indicates localized clots and/or vertical layers of blood 1 mm or greater in thickness. We defined low-grade SAH based on the previously mentioned clinical criteria and on the modified Fisher grade for vasospasm, which ranged from 0 to 3. Intraventricular hemorrhage (IVH) was classified as present or absent.

Sensitivity was measured by dividing the number of patients with SAH detected on FLAIR imaging, T2\* imaging, or CT alone by the total number of patients with SAH.

As proposed by Mitchell et al,<sup>16</sup> an additional measure of the sensitivity of the imaging methods relative to each other is presented. The presence or absence of blood was recorded on all scans at the 26 previously mentioned locations. To assess the sensitivity of FLAIR imaging, T2\* imaging, or CT, a location was assumed to contain blood if it was found to be positive on any of the MRI sequences or CT. The proportion of this total found to be positive using FLAIR imaging, T2\* imaging, or CT alone was taken as a guide to

the sensitivity of a particular imaging modality relative to the others. We referred to this additional measure as locational sensitivity.

We used nonparametric tests to evaluate different scores of sequences to compare related samples (Friedman test). To compare the methods with each other, we used multiple comparison (Conover). The methods were compared by the McNemar test to detect ventricle hemorrhage, corresponding to a  $\chi^2$  test of dependent samples (binare answer).<sup>18-20</sup> The significance level was 0.05.

### RESULTS

In the acute SAH group, the sensitivities according to the imaging modality were as follows: 100% for FLAIR imaging, 71.8% for CT, and 37.5% for T2\* imaging; in the subacute group, they were as follows: 100% for FLAIR imaging, 50% for CT, and 30% for T2\* imaging (Fig. 1). Computed tomography had a considerable decrease in sensitivity in the subacute SAH group (Fig. 2).

The locational sensitivities were also superior on FLAIR images, followed by CT and T2\* sequences, respectively. Fluid-attenuated inversion recovery imaging was superior to CT in detecting SAH in 15 out of the 26 evaluated regions (Table 1; Fig. 3).

The modified Fisher scale used to compare the different methods demonstrated the superiority of the FLAIR images. The mean modified Fisher grades were as follows: 2.7 for FLAIR imaging, 2.1 for CT, and 1.8 for T2\* imaging. Comparing FLAIR sequences with CT, the modified Fisher

scale score increased in 21 patients, decreased in 6 patients (but did not exclude SAH), and was the same in 15 patients.

The mean of locations (total of 26 locations) in which SAH was detected in each sequence were as follows: 23.5 for FLAIR imaging, 12.9 for CT, and 3.5 for T2\* imaging. Based on these data, the FLAIR sequence was superior in evaluating the extension of hemorrhage.

We demonstrated SAH on T2\* images as areas of hypointensity in the SAS. The T2\* sequence became useful in 15 (35.7%) patients with more extensive SAH, clot, or hemorrhage in the lateral ventricles, corroborating FLAIR findings (Table 2; Fig. 4).

The sites of low-grade hemorrhage were more frequent in the SAS of the parietal and occipital lobes and in the convexity sulci (see Table 1). There was no misdiagnosis of SAH in the control group (no false-positive results).

### DISCUSSION

We compare the sensitivity of FLAIR and T2\* sequences with CT scans for the diagnosis and localization of acute and subacute low-grade SAH. Thus, it is presumed that SAH was diagnosed with 1 of the 3 methods for every patient. The lack of lumbar puncture procedures in our sample should be considered a limitation of our study. There was no point in performing cerebrospinal fluid (CSF) analysis in our patients, however, because all of them underwent CT and MRI examinations first, with the FLAIR sequence confirming the presumptive diagnosis of SAH in all except 3 individuals. Only these 3 patients underwent a lumbar

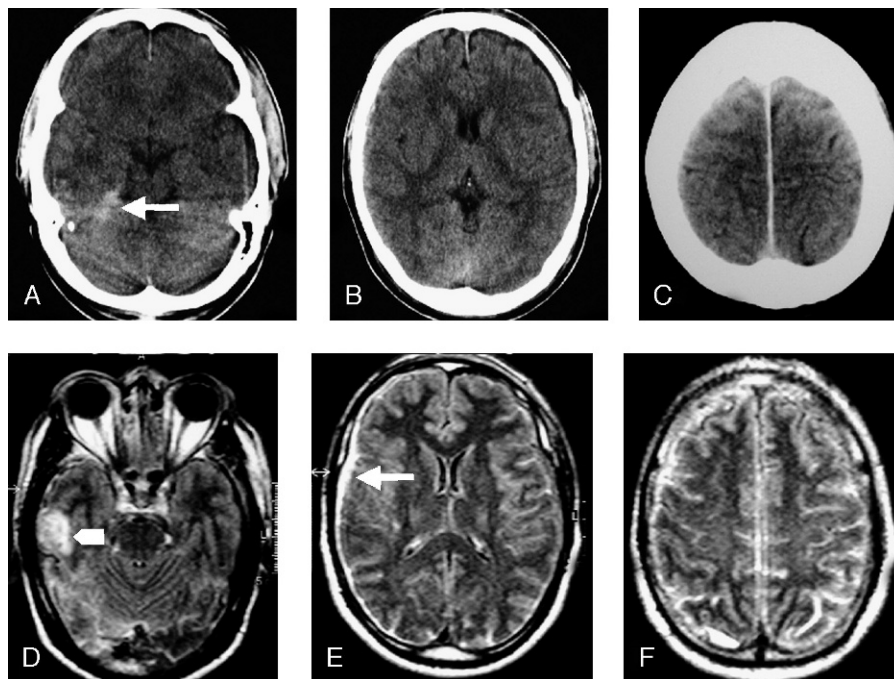


**FIGURE 1.** Subarachnoid hemorrhage in a 52-year-old man 1 day after minor head trauma. A-C, Nonenhanced CT scans show SAH as a hyperattenuating area at the right tentorium (arrow in A) and effacement of right hemispheric sulci. Fluid-attenuated inversion recovery images also show a cortical contusion at the right temporal lobe (arrowhead in D), subdural parieto-occipital hematoma (arrow in E), and SAH as diffuse hyperintensity areas in the frontal and parietal sulci (E, F). All these findings were underestimated on T2\* images (not shown).

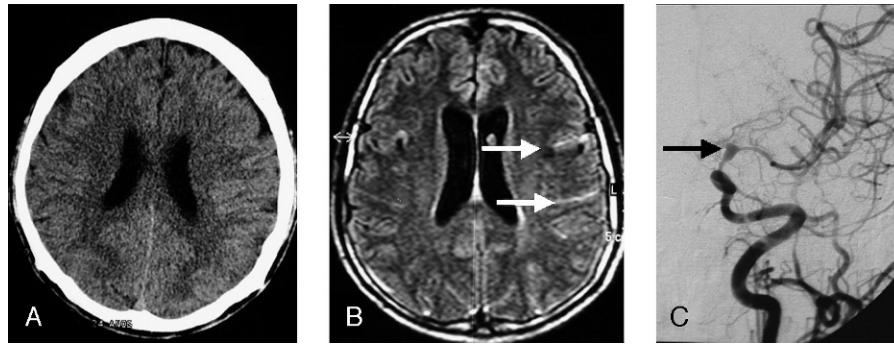


**FIGURE 2.** Subacute SAH in a 24-year-old woman with an 8-day headache. A, Results of a nonenhanced CT scan are normal. B, Fluid-attenuated inversion recovery image shows SAH as hyperintensity areas at the left frontoparietal sulci (arrows). C, Digital angiography shows a ruptured aneurysm at the bifurcation of the left internal carotid artery (arrow) and associated vasospasm.

puncture procedure according to clinical judgment, and as mentioned previously, none of them presented with SAH after CSF analysis (no false-negative results). We clearly demonstrated acute and subacute SAH as areas of hyperintensity on FLAIR sequences, with a sensitivity superior to that of CT and T2\* sequences.

Traumatic SAH frequently occurs in patients with brain injury, but it is difficult to detect and grade based on CT scans.<sup>21</sup> Our traumatic SAH group included only individuals

with minor head trauma, and our spontaneous SAH group included subjects with severe headache that led to a suspicion of SAH with minimal clinical abnormalities. Both of our groups proved to be useful models in vivo to test the discrepancy among imaging techniques in low-grade SAH, because these patients were previously healthy individuals with no history of coagulation disturbances.

The clinical hallmark of spontaneous SAH is a sudden explosive headache, but this is a nonspecific feature in the

**TABLE 1.** Locational Sensitivities of CT Scans and FLAIR and T2\* MRI Sequences in 42 Patients With Low-Grade SAH in 26 Locations

Locations	No. Patients	Multiple Comparisons		
		CT × T2* P	CT × FLAIR P	T2* × FLAIR P
Magna cistern	9	>0.999	0.046*	0.046*
Prepontine cistern	18	0.735	0.030*	0.013*
Superior cerebellar cistern	12	0.775	0.210	0.332
Perimesencephalic cistern	18	0.917	0.051	0.040*
Interpeduncular cistern	18	0.910	0.049*	0.038*
Suprasellar cistern	15	0.834	0.146	0.097
Cerebellar sulci	10	>0.999	0.033*	0.033*
Right cerebellopontine cistern	10	0.841	0.111	0.074
Left cerebellopontine cistern	12	0.952	0.043*	0.037*
Right tentorium	7	0.818	0.463	0.613
Left tentorium	5	0.438	0.332	0.846
Frontal interhemispheric sulci	12	0.080	0.909	0.101
Parietal interhemispheric sulci	15	0.012*	0.355	0.107
Occipital interhemispheric sulci	24	0.004*	0.741	0.012*
Right convexity sulci	26	0.488	<0.001*	<0.001*
Right temporal convexity sulci	22	0.639	0.003*	<0.001*
Right frontal convexity sulci	20	0.385	0.021*	0.001*
Right parietal convexity sulci	24	0.676	0.001*	<0.001*
Right occipital convexity sulci	29	0.628	<0.001*	<0.001*
Left convexity sulci	27	0.388	<0.001*	<0.001*
Left temporal convexity sulci	24	0.962	0.002*	0.001*
Left frontal convexity sulci	21	0.590	0.014*	0.003*
Left parietal convexity sulci	29	0.661	<0.001*	<0.001*
Left occipital convexity sulci	31	0.902	<0.001*	<0.001*
Right Sylvian fissure	11	0.756	0.354	0.217
Left Sylvian fissure	13	0.640	0.104	0.243

\*P < 0.05.

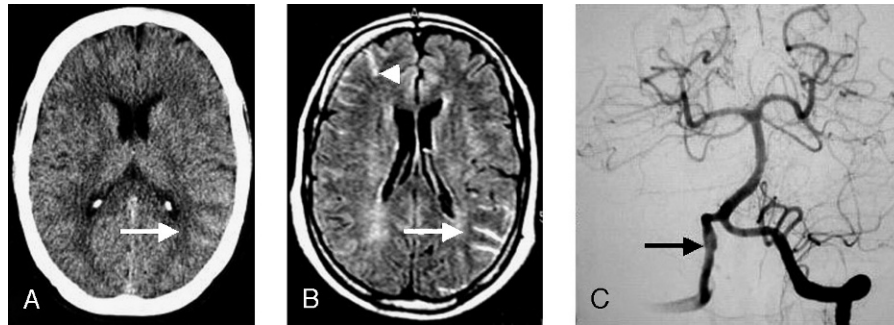


**FIGURE 3.** Hyperacute SAH in a 60-year-old woman with headache of less than 3 hours' duration. A, Nonenhanced CT scan shows only slight hyperattenuating foci at the left parietal sulci (arrow). B, Fluid-attenuated inversion recovery shows a greater amount of SAH as hyperintensity areas at the left parietal sulci (arrow) and at the right frontal sulci (arrowhead). C, Digital angiography shows a dissection at the right vertebral artery (arrow).

diagnosis of this serious condition. In general practice, if explosive headache is the only symptom, the chance of SAH being the cause is only 10%.<sup>22</sup> Despite this, headache (“sentinel headache”) or cranial nerve palsy may occur in an isolated manner at first, and low-grade SAH must be suspected and promptly excluded in all these individuals.<sup>1,4,23,24</sup> A CT scan is mandatory in all such patients, to be followed by lumbar puncture if the CT results are negative. The cause of spontaneous SAH is a ruptured aneurysm in 85% of cases.<sup>25</sup> Approximately 20% to 50% of patients with a ruptured aneurysm have minor hemorrhage or a warning leak, often with atypical clinical features, 1 to 6 weeks before a major episode of SAH.<sup>23</sup> When aneurysmal rebleeding has occurred, patients are usually in a deteriorated condition and present with a worse prognosis.<sup>1,3,9</sup> Occlusion of the aneurysm is the only effective action to prevent an increase in the morbidity and mortality rates.<sup>5</sup>

Patients with low-grade SAH, who are the most likely to receive an incorrect clinical diagnosis, are also more likely to have negative results on CT.<sup>1</sup> The appearance of SAH on CT relies on electron density in a tissue and depends on the attenuation values of the blood in the CSF spaces.<sup>16</sup> It is linearly related to hematocrit and hemoglobin levels.<sup>26</sup> Hyperacute hemorrhage (<2 hours after ictus) may not be seen, because fresh blood has the same electron density as brain and other soft tissues. With time, there is reabsorption of serum of the hematoma and an increase in hematocrit and electron densities from local packed cells, making acute SAH visible as hyperattenuating areas on nonenhanced CT scans. After this, CSF circulation redistributes the hemorrhage, and reabsorption of serum is followed by reabsorption of the

protein component; consequently, the sensitivity of CT continuously declines.<sup>16</sup> We believe that CSF circulation and dilution effects of protein in CSF are the most important factors for missing a minor leak on CT scans.

Magnetic resonance imaging signal is based on proton density and depends on the difference in the T1 and T2 relaxation times between SAH, CSF, and brain parenchyma.<sup>27</sup> Magnetic resonance imaging field strength, sequence parameters, the specific intracranial compartment affected, and different stages of hemoglobin oxygenation and its products are the most important variables having profound effects on the MRI signal of intracranial hemorrhage.

Subarachnoid hemorrhage differs from intraparenchymal hemorrhage because of different levels of oxyhemoglobin in CSF,<sup>28</sup> mainly attributable to its arterial origin.<sup>29</sup> Subarachnoid hemorrhage is also different from other extra-axial hemorrhage because of its mixture with CSF and the slower progression from one stage of hemoglobin oxygenation to the next.<sup>29</sup> Grossman et al<sup>30</sup> reported that the high oxygen tension of CSF imposes restrictions on the formation of paramagnetic deoxyhemoglobin in SAH. The protein component in SAH produces high T2 signal, which is swamped by the high signal from CSF on T2-weighted images.<sup>11,30</sup> It has been accepted that it is difficult to detect acute SAH with standard T1- and T2-weighted spin echo sequences and that these techniques are less informative than CT.<sup>12,31</sup>

Magnetic resonance imaging, including FLAIR and T2\* sequences, offers an improvement in the detection of SAH, because FLAIR sequences evaluate an increase in CSF cellularity and protein content and T2\* sequences evaluate

**TABLE 2.** Comparison of FLAIR and T2\* MRI Sequences With CT Scans in the Detection of IVH

Locations	Imaging Modality			Multiple Comparisons		
	CT n (%)	T2* n (%)	FLAIR n (%)	CT × T2* P	CT × FLAIR P	T2* × FLAIR P
Third ventricle	1 (2.1)	2 (4.3)	11 (23.4)	>0.999	0.002*	0.004*
Fourth ventricle	1 (2.1)	2 (4.3)	16 (34.0)	>0.999	<0.001*	<0.001*
Right lateral ventricle	2 (4.3)	4 (8.5)	5 (10.6)	0.500	0.250	>0.999
Left lateral ventricle	3 (6.4)	3 (6.4)	6 (12.8)	>0.999	0.375	0.250

\*P < 0.05.

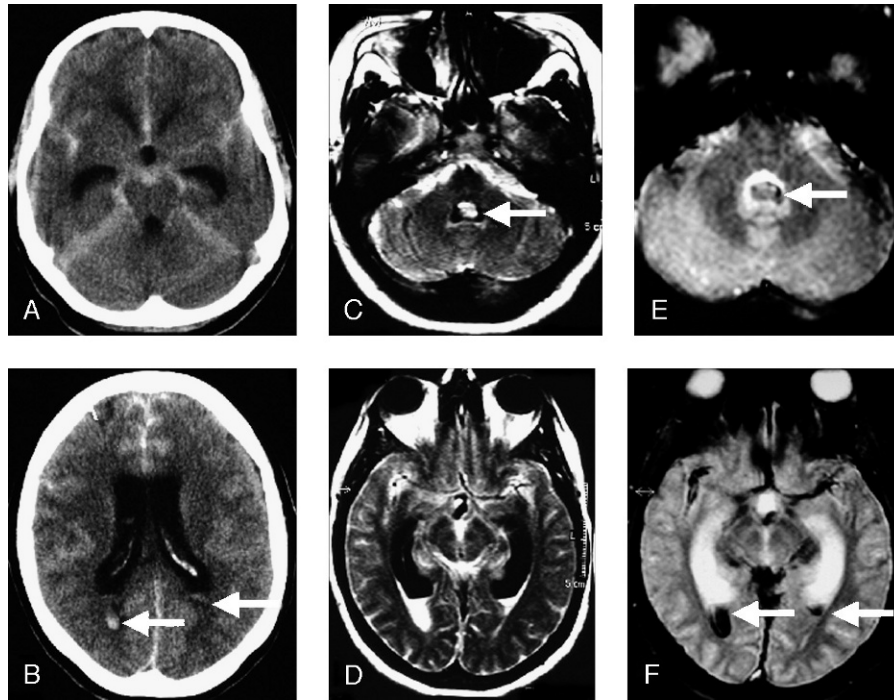


**FIGURE 4.** Acute SAH in a 50-year-old woman headache of 2 days' duration. A, B, Nonenhanced CT scans show diffuse SAH as areas of high attenuation at the basal cisterns, Sylvian and interhemispheric fissures, and tentorial and frontoparietal sulci. Intraventricular hemorrhage is also seen at the occipital horns (arrows in B). C, D, Fluid-attenuated inversion recovery show more extensive SAH and also demonstrates blood at the fourth ventricle (arrow in C), which is not shown on CT scans. E, F, T2-weighted gradient echo images were useful to confirm blood at the fourth and lateral ventricles as areas of hypointensity (arrows) but failed to demonstrate SAH at the temporal and occipital sulci.

the paramagnetic effect of iron. Both depend on the appearance of hemoglobin and its breakdown products.<sup>16</sup> Based on the first report of FLAIR by Hajnal et al,<sup>32</sup> several recent studies have suggested that this is the most sensitive MRI sequence for the detection of SAS involvement and for the demonstration of brain abnormalities, particularly those adjacent to CSF,<sup>33–35</sup> and it has been used by some authors to reveal SAH.<sup>13,14,27,36</sup> The existence of plasma protein within the SAS shortens the T1 relaxation time of bloody CSF,<sup>27,37,38</sup> leading to hyperintensity of the hemorrhage on FLAIR sequences, as opposed to the SAS hypointensity determined by signal suppression of free water by the inversion recovery technique.<sup>6,13,14,36</sup> Heavy T2 weighting preferentially suppresses signal intensity from the brain parenchyma compared with bloody CSF, because the T2 relaxation time of some bloody CSF is longer than that of the brain parenchyma.<sup>27</sup> Because the FLAIR sequence is heavily T2 weighted, it allows the signal intensity from bloody CSF to exceed that of brain parenchyma.<sup>27</sup> Based on the previous explanations, this combination of the T1 and T2 effects of bloody CSF can be demonstrated on FLAIR images, explaining, at least in part, its superior sensitivity when compared with T2\* and CT images.

Noguchi et al<sup>27</sup> have demonstrated that FLAIR imaging is more sensitive than CT in the detection of a small amount of acute SAH diluted in CSF. It has been proven that different protein concentration thresholds can affect CSF signal

intensity on FLAIR sequences.<sup>39</sup> Recently, Mohamed et al<sup>38</sup> have suggested, in a comparison *in vivo*, that there would be a threshold of blood concentration in the SAS that would have to be exceeded for bloody CSF to become visible on FLAIR sequences.

In several instances, we detected SAH on CT, but FLAIR imaging was able to demonstrate blood not only in the same locations revealed on CT but in several others not previously suspected, allowing better assessment of the extent of hemorrhage, which is demonstrated by the increase in locational sensitivities. Comparing FLAIR imaging with CT, the modified Fisher scale score increased in 21 patients, decreased in 6 patients (but did not exclude SAH), and was the same in 15 patients.

We assume that the modified Fisher scale decreased in some cases because FLAIR imaging is more trustworthy than CT. Our results are in agreement with those of previous reports.<sup>13,15,27,40</sup> These results diverge from those reported by Mitchell et al,<sup>16</sup> but different parameters used here limit a reliable comparison.

Sulcal and intraventricular CSF hyperintensity on FLAIR images may also be seen in conditions other than SAH, including ruptured dermoid, meningitis, meningeal metastasis, and disruption of the blood-brain barrier causing leakage of protein and gadolinium chelates in the SAS on post-contrast images.<sup>34,41,43</sup> These abnormalities can be differentiated from SAH based on clinical information, use of

gadolinium-enhanced acquisitions, and some other peculiarities of these conditions, however. Sulcal hyperintensity on FLAIR images is a nonspecific pattern that can occur even without any CSF abnormality.<sup>44</sup> This finding is particularly associated with vascular diseases such as stroke, venous thrombosis, dural arteriovenous fistula, and mass effect. A special condition is related to dural venous thrombosis and arteriovenous fistulae, where the increase of venous pressure presumably causes increased blood flow and an alteration in vascular hemodynamics with slow flow. This was reported by Taoka et al<sup>44</sup> in 2 different patients and could determine a special type of sulcal hyperintensity on FLAIR sequences and mild hypointensity on T2\* sequences, suggesting an increase in local field inhomogeneity. This situation must be recognized to avoid SAH misdiagnosis.

Different mechanisms, including diffuse cerebral edema, may show increased attenuation in the perimesencephalic cisterns and along the tentorial surface resembling SAH on nonenhanced CT scans (pseudo-SAH).<sup>45,46</sup> This is not a problem for any MRI sequence, however.

Cerebrospinal fluid flow and venous blood artifacts on FLAIR images demonstrated as areas of hyperintensity in basal cisterns and in the third and fourth ventricles when one uses high field strengths can produce IVH misdiagnosis in some instances.<sup>31,47,48</sup>

We demonstrated that FLAIR imaging was superior to CT in detecting minor IVH, but this particular discussion is limited by the small number of IVHs in our sample. Intraventricular hemorrhage was not falsely diagnosed in any of the control subjects on FLAIR sequences. Our results agree with those reported by Bakshi et al,<sup>48</sup> who consider MRI studies, including FLAIR imaging, to be an effective and reliable technique in the detection of acute and subacute IVH and coexisting SAH.

Intraventricular CSF pulsation artifact on FLAIR sequences could represent a problem in the interpretation of this sequence.<sup>31</sup> This most likely results from inflow artifact caused by inversion delay and ghosting effects. It is common in adults and is associated with advancing age and increasing ventricular size.<sup>47</sup> Despite this, FLAIR sequences have shown high sensitivity and specificity in identifying IVH in lateral ventricles.<sup>48</sup> To study subacute hemorrhage, particularly in the third and fourth ventricles, Bakshi et al<sup>48</sup> recommend caution and acquisition of conventional MRI sequences to complement FLAIR sequences. In our sample, IVH was also conspicuously defined on T2\* images and it helped to confirm these findings on FLAIR sequences. The small number of cases in our study hinders comparative analysis between T2\* and FLAIR sequences, however. We believe that they should be used together.

Both iron forms ( $\text{Fe}^{3+}$  and  $\text{Fe}^{2+}$ ) are paramagnetic. The presence of these paramagnetic substances in the CSF leads to perturbation in the magnetic field, which becomes visible on MRI, particularly on T2\* sequences, even in the acute stage of SAH.<sup>16</sup> Subarachnoid hemorrhage on T2\* images was demonstrated as areas of hypointensity in the SAS but was only visible in cases of more extensive hemorrhage or clot because it depends predominantly on the amount of iron in a voxel.

In the infratentorial compartment, FLAIR imaging was superior to CT and T2\* imaging in detecting abnormalities suggestive of SAH. Subarachnoid hemorrhage in the infratentorial compartment (including the basal cisterns) near the skull base was particularly difficult to see using T2\*, probably because of susceptibility effects from the skull-base and low-grade hemorrhage. Fiebach et al<sup>5</sup> have reported similar difficulties in interpreting T2\* sequences. Noguchi et al<sup>14</sup> demonstrated better conspicuity on FLAIR sequences than on CT scans in the detection of infratentorial SAH, presumably because of beam-hardening artifacts on CT. In our sample, FLAIR imaging was superior, probably because of its capability to detect an increase in protein concentration and cellularity in the CSF without interference of paramagnetic substances or perturbation in local magnetic fields.

Neither sedation nor anesthesia was used in any of our patients. To avoid CSF hyperintensities in the SAS on FLAIR images, we routinely use 50% supplemental oxygen, allowing complete suppression of CSF signal in patients who need assisted ventilation, thus avoiding misdiagnosis.<sup>49,50</sup>

An interesting finding from our sample is related to the site of low-grade hemorrhage. It was more frequent in the SAS of the posterior lobes and in the convexity sulci, probably determined by gravitational effects related to bed restriction and recirculation of blood in CSF that carries it to convexity SAS.

FLAIR and T2\* sequences did not demonstrate SAH in the control group or in the 3 patients with normal lumbar puncture results (no false-positive results). These sequences can be performed on standard MRI scanners, and they are able to supplement CT in the detection of low-grade SAH. According to Mitchell et al,<sup>16</sup> MRI is also useful to study patients presenting with atypical symptoms, where FLAIR and T2\* imaging may be used as additional tests when CT and lumbar puncture give inconclusive or contradictory results. We consider that they also represent an option when CT is normal or inconclusive and lumbar puncture cannot be performed according to clinical judgment. We believe that these sequences are important tools to exclude differential diagnoses such as venous thrombosis, arterial dissection, and ruptured vascular malformation among others, allowing an adequate differential diagnosis for most SAH patients and avoiding unnecessary lumbar puncture procedures.

Imaging provides visual detection of SAS abnormalities, but CSF examination provides a quantitative analysis that measures the concentration of blood and estimates all SAS. Our study has several limitations, including the magnet field strength, absence of correlation with CSF analysis, and limited number of patients. We considered that a 1.0-T magnet could interfere with T2\* imaging results.

FLAIR and T2\* images do not allow us to discard lumbar puncture, and CT remains the imaging procedure of choice for the initial evaluation of patients clinically suspected of SAH. Currently, MRI is being used as a standard protocol for the initial investigation of acute stroke-like symptoms in several stroke centers around the world, and it is important to define precise parameters for the interpretation of MRI in the detection of intracranial hemorrhage.<sup>51,52</sup>

## CONCLUSIONS

The FLAIR sequence showed the highest sensitivity in the detection and localization of acute and subacute low-grade SAH, representing a potential tool for clinical investigation. It should be used in cases of suspected SAH with normal or inconclusive CT scans or in patients who are not suitable candidates for lumbar puncture. The FLAIR sequence proved to be the most useful imaging modality in the detection of minor SAH, and the T2\* sequence could be complementary to the FLAIR sequence, particularly to confirm IVH. Computed tomography scans are useful to detect acute SAH, but they can have normal results in low-grade, infratentorial, or subacute SAH.

## REFERENCES

- Edlow JA, Caplan LR. Avoiding pitfalls in the diagnosis of subarachnoid hemorrhage. *N Engl J Med*. 2000;342:29–36.
- Kowalski RG, Claassen J, Kreiter KT, et al. Initial misdiagnosis and outcome after subarachnoid hemorrhage. *JAMA*. 2004;291:866–869.
- Mayer PL, Awad IA, Todor R, et al. Misdiagnosis of symptomatic cerebral aneurysm. Prevalence and correlation with outcome at four institutions. *Stroke*. 1996;27:1558–1563.
- Linn FH, Rinkel GJ, Algra A, et al. Headache characteristics in subarachnoid haemorrhage and benign thunderclap headache. *J Neurol Neurosurg Psychiatry*. 1998;65:791–793.
- Fiebach JB, Schellinger PD, Geletneky K, et al. MRI in acute subarachnoid haemorrhage: findings with a standardised stroke protocol. *Neuroradiology*. 2004;46:44–48.
- Adams HP Jr, Jergenson DD, Kassell NF, et al. Pitfalls in the recognition of subarachnoid hemorrhage. *JAMA*. 1980;244:794–796.
- Morgenstern LB, Luna-Gonzales H, Huber JC Jr, et al. Worst headache and subarachnoid hemorrhage: prospective, modern computed tomography and spinal fluid analysis. *Ann Emerg Med*. 1998;32:297–304.
- Vermeulen M, van Gijn J. The diagnosis of subarachnoid haemorrhage. *J Neurol Neurosurg Psychiatry*. 1990;53:365–372.
- Leblanc R. The minor leak preceding subarachnoid hemorrhage. *J Neurosurg*. 1987;66:35–39.
- Jakobsson KE, Saveland H, Hillman J, et al. Warning leak and management outcome in aneurysmal subarachnoid hemorrhage. *J Neurosurg*. 1996;85:995–999.
- Chakeres DW, Bryan RN. Acute subarachnoid hemorrhage: in vitro comparison of magnetic resonance and computed tomography. *AJNR Am J Neuroradiol*. 1986;7:223–228.
- Atlas SW. MR imaging is highly sensitive for acute subarachnoid hemorrhage not? *Radiology*. 1993;186:319–322.
- Noguchi K, Ogawa T, Inugami A, et al. MR of acute subarachnoid hemorrhage: a preliminary report of fluid-attenuated inversion-recovery pulse sequences. *AJNR Am J Neuroradiol*. 1994;15:1940–1943.
- Noguchi K, Ogawa T, Inugami A, et al. Acute subarachnoid hemorrhage: MR imaging with fluid-attenuated inversion recovery pulse sequences. *Radiology*. 1995;196:773–777.
- Woodcock RJ Jr, Short J, Do HM, et al. Imaging of acute subarachnoid hemorrhage with a fluid-attenuated inversion recovery sequence in an animal model: comparison with non-contrast-enhanced CT. *AJNR Am J Neuroradiol*. 2001;22:1698–1703.
- Mitchell P, Wilkinson ID, Hoggard N, et al. Detection of subarachnoid haemorrhage with magnetic resonance imaging. *J Neurol Neurosurg Psychiatry*. 2001;70:205–211.
- Fisher CM, Kistler JP, Davis JM. Relation of cerebral vasospasm to subarachnoid hemorrhage visualized by computerized tomographic scanning. *Neurosurgery*. 1980;6:1–9.
- Bussab WO, Morettin PA. *Estatística Básica*. São Paulo, SP: Atual, 1987.
- Armitage P, Berry G. *Statistical Methods in Medical Research*. Oxford: Blackwell Science, 1994.
- Conover WJ. *Practical Nonparametric Statistics*. New York: John Wiley and Sons, 1980.
- Mattioli C, Beretta L, Gerevini S, et al. Traumatic subarachnoid hemorrhage on the computerized tomography scan obtained at admission: a multicenter assessment of the accuracy of diagnosis and the potential impact on patient outcome. *J Neurosurg*. 2003;98:37–42.
- Linn FH, Wijdicks EF, van der Graaf Y. Prospective study of sentinel headache in aneurysmal subarachnoid haemorrhage. *Lancet*. 1994;344:590–593.
- Hauerberg J, Andersen BB, Eskesen V, et al. Importance of the recognition of a warning leak as a sign of a ruptured intracranial aneurysm. *Acta Neurol Scand*. 1991;83:61–64.
- Chrysikopoulos H, Papanikolaou N, Pappas J, et al. Acute subarachnoid haemorrhage: detection with magnetic resonance imaging. *Br J Radiol*. 1996;69:601–609.
- van Gijn J, Rinkel GJ. Subarachnoid haemorrhage: diagnosis, causes and management. *Brain*. 2001;124:249–278.
- Norman D, Price D, Boyd D, et al. Quantitative aspects of computed tomography of the blood and cerebrospinal fluid. *Radiology*. 1977;123:335–338.
- Noguchi K, Seto H, Kamisaki Y, et al. Comparison of fluid-attenuated inversion-recovery MR imaging with CT in a simulated model of acute subarachnoid hemorrhage. *AJNR Am J Neuroradiol*. 2000;21:923–927.
- Bradley WG Jr, Schmidt PG. Effect of methemoglobin formation on the MR appearance of subarachnoid hemorrhage. *Radiology*. 1985;156:99–103.
- Parizel PM, Makkat S, van Miert E, et al. Intracranial hemorrhage: principles of CT and MRI interpretation. *Eur Radiol*. 2001;11:1770–1783.
- Grossman RI, Kemp SS, Ip CY, et al. The importance of oxygenation in the appearance of acute subarachnoid hemorrhage on high field magnetic resonance imaging. *Acta Radiol Suppl*. 1986;369:56–58.
- Wiesmann M, Mayer TE, Yousry I, et al. Detection of hyperacute subarachnoid hemorrhage of the brain by using magnetic resonance imaging. *J Neurosurg*. 2002;96:684–689.
- Hajnal JV, Bryant DJ, Kasuboski L, et al. Use of fluid-attenuated inversion recovery (FLAIR) pulse sequences in MRI of the brain. *J Comput Assist Tomogr*. 1992;16:841–844.
- Saleh A, Wenserski F, Cohnen M, et al. Exclusion of brain lesions: is MR contrast medium required after a negative fluid-attenuated inversion recovery sequence? *Br J Radiol*. 2004;77:183–188.
- Maeda M, Yagishita A, Yamamoto T, et al. Abnormal hyperintensity within the subarachnoid space evaluated by fluid-attenuated inversion-recovery MR imaging: a spectrum of central nervous system diseases. *Eur Radiol*. 2003;13(Suppl 4):L192–L201.
- Kates R, Atkinson D, Brant-Zawadzki M. Fluid-attenuated inversion recovery (FLAIR): clinical prospectus of current and future applications. *Top Magn Reson Imaging*. 1996;8:389–396.
- Noguchi K, Ogawa T, Seto H, et al. Subacute and chronic subarachnoid hemorrhage: diagnosis with fluid-attenuated inversion-recovery MR imaging. *Radiology*. 1997;203:257–262.
- Bradley WG. MR appearance of hemorrhage in the brain. *Radiology*. 1993;189:15–26.
- Mohamed M, Heasly DC, Yagmurlu B, et al. Fluid-attenuated inversion recovery MR imaging and subarachnoid hemorrhage: not a panacea. *AJNR Am J Neuroradiol*. 2004;25:545–550.
- Melhem ER, Jara H, Eustace S. Fluid-attenuated inversion recovery MR imaging: identification of protein concentration thresholds for CSF hyperintensity. *AJR Am J Roentgenol*. 1997;169:859–862.
- Ogawa T, Inugami A, Shimosegawa E, et al. Subarachnoid hemorrhage: evaluation with MR imaging. *Radiology*. 1993;186:345–351.
- Singer MB, Atlas SW, Drayer BP. Subarachnoid space disease: diagnosis with fluid-attenuated inversion-recovery MR imaging and comparison with gadolinium-enhanced spin-echo MR imaging-blinded reader study. *Radiology*. 1998;208:417–422.
- Tsuchiya K, Inaoka S, Mizutani Y, et al. Fast fluid-attenuated inversion-recovery MR of intracranial infections. *AJNR Am J Neuroradiol*. 1997;18:909–913.
- Dechambre SD, Duprez T, Grandin CB, et al. High signal in cerebrospinal fluid mimicking subarachnoid haemorrhage on FLAIR following acute stroke and intravenous contrast medium. *Neuroradiology*. 2000;42:608–611.

44. Taoka T, Yuh WT, White ML, et al. Sulcal hyperintensity on fluid-attenuated inversion recovery MR images in patients without apparent cerebrospinal fluid abnormality. *AJR Am J Roentgenol*. 2001;176:519–524.
45. Given CA II, Burdette JH, Elster AD, et al. Pseudo-subarachnoid hemorrhage: a potential imaging pitfall associated with diffuse cerebral edema. *AJNR Am J Neuroradiol*. 2003;24:254–256.
46. Rabinstein AA, Pittock SJ, Miller GM, et al. Pseudosubarachnoid haemorrhage in subdural haematoma. *J Neurol Neurosurg Psychiatry*. 2003;74:1131–1132.
47. Bakshi R, Caruthers SD, Janardhan V, et al. Intraventricular CSF pulsation artifact on fast fluid-attenuated inversion-recovery MR images: analysis of 100 consecutive normal studies. *AJNR Am J Neuroradiol*. 2000;21:503–508.
48. Bakshi R, Kamran S, Kinkel PR, et al. Fluid-attenuated inversion-recovery MR imaging in acute and subacute cerebral intraventricular hemorrhage. *AJNR Am J Neuroradiol*. 1999;20:629–636.
49. Anzai Y, Ishikawa M, Shaw DW, et al. Paramagnetic effect of supplemental oxygen on CSF hyperintensity on fluid-attenuated inversion recovery MR images. *AJNR Am J Neuroradiol*. 2004;25:274–279.
50. Braga FT, da Rocha AJ, Hernandez Filho G, et al. Relationship between the concentration of supplemental oxygen and signal intensity of CSF depicted by fluid-attenuated inversion recovery imaging. *AJNR Am J Neuroradiol*. 2003;24:1863–1868.
51. Perl J, Tkach JA, Porras-Jimenez M, et al. Hemorrhage detected using MR imaging in the setting of acute stroke: an in vivo model. *AJNR Am J Neuroradiol*. 1999;20:1863–1870.
52. Kidwell CS, Chalela JA, Saver JL, et al. Comparison of MRI and CT for detection of acute intracerebral hemorrhage. *JAMA*. 2004;292:1823–1830.